Influence of film thickness on structural and optical properties of nanocrystalline tellurium films

P. DEEPAK RAJ, R. VENKATESAN, P. DHIVYA, S. GAYATHRI, M. SRIDHARAN*
Functional Nanomaterials & Devices Lab, Centre for Nanotechnology &Advanced Biomaterials and School of Electrical & Electronics Engineering, SASTRA University, Thanjavur – 613 401, India

Nanocrystalline tellurium (Te) thin films of different thickness were deposited onto thoroughly cleaned glass substrates using conventional thermal evaporation technique. The structural, morphological and the optical properties of the samples were investigated using X-ray diffraction (XRD), field-emission scanning electron microscopy (FE-SEM) and UV-Vis spectroscopy, respectively. The grain size values of the films were increased on increasing the thickness while the strain values were decreased. The optical band gap of the films were varied between 3.92 – 1.3 eV as analyzed by UV-Vis spectroscopy. The refractive index of the film was increasing with increase in thickness. The results were correlated to the decrease in the lattice defects on growing thicker films.

(Received February 12, 2013; accepted July 10, 2014)

Keywords: Tellurium films, Thermal evaporation, X-ray diffraction, Optical properties

1. Introduction

Te thin films drew attention of many researchers for the past three decades towards the application in the areas of solar cell, infrared detectors, optical information storage etc., because of its dielectric and conducting feature. Besides these films play a major role in the passive radiative cooling system as shields [1] and also it can be used in gas sensing due to its superior response towards the toxic gases at room temperature. Various deposition techniques such as reactive magnetron sputtering [1-3], thermal evaporation [4-11], spray pyrolysis [12], plasma activated reactive bias assisted deposition [13] and Sol gel [14] has been used to synthesize the Te thin films.

Balasubramaniam *et. al.* [4] deposited the Te (Al-Te-Al) thin films using thermal evaporation technique and studied its conduction and dielectric properties in the frequency range of 1-100 MHz in various temperatures. M. Rusu *et. al.* [5] deposited stratified tellurium films using the thermal evaporation technique and studied its optical (in the IR region) and electrical properties. Alexis De Vos *et. al.* [6] deposited the film using the thermal evaporation technique and studied the influence of deposition rate on the electrical properties of films. Janan H. Saadee *et. al*. [12] deposited the Te thin films using the spray pyrolysis technique at the substrate temperature of 450 °C and studied its optical properties.

Among different deposition techniques, thermal evaporation is economic, ease of operation and suitable for uniform large area coating. Since, not many reports are available for the influence of film thickness on the optical properties of vacuum evaporated Te films, in the present work we have deposited Te thin films on glass substrates using thermal evaporation technique and the effect of film thickness on the structural, morphological and the optical properties were investigated.

2. Experimental method

Te thin films were prepared by evaporating tellurium ingot (Sigma Aldrich, 99.999% purity) using molybdenum boat as the evaporation source. The films were deposited on to cleaned glass substrates of dimension 2 × 1 cm^2. The substrates were thoroughly cleaned in double distilled water, acetone and ethanol using an ultrasonicator for 10 minutes in each solution. The deposition chamber was evacuated to a base pressure of 1.3 × 10^{-5} mbar. For all depositions, the substrate temperature was maintained at 100 °C, source to substrate distance was maintained as 20 cm and the working pressure was maintained at 4 × 10^{-5} mbar. In order to obtain Te films with different thicknesses the depositions were carried out for 5, 10 and 15 min. The film thicknesses (t) measured by stylus probe technique were 350, 750 and 1050 nm respectively. The film deposited for 5 min was found to be transparent and with the increase in the deposition time the thickness of the film increased which made the film opaque as shown in Fig. 1. The as-deposited films were employed for different characterization.

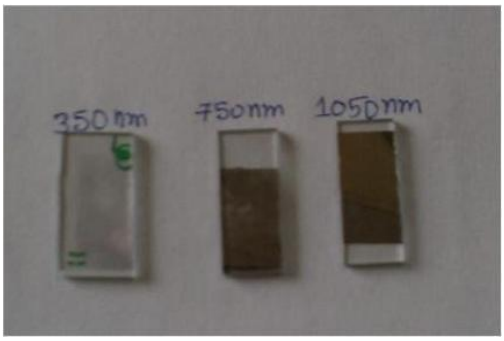

Fig. 1. Photographic image of Te films of different thickness.

The microstructure of the Te films was investigated using XRD (Rigaku, Ultima III, Japan) operated at 60 kV and 60 mA with CuK_α (1.54 Å) radiation. The surface morphology of the films was studied using FE-SEM (JEOL-JSM 6701F, Japan) using energy of 3 kV and operated at a working distance of 6.7 – 6.9 mm. The optical properties of the films were determined using the absorbance spectra taken from UV-Visible spectroscopy (Perkin Elmer - Lambda 35) in the spectral range between the 200 - 800 nm.

Table 1. Microstructural parameters of Te films with different thicknesses.

Thickness (nm)	2θ (°)	$\beta_{2\theta}$ (radian)	Interplanar spacing (d) (Å)	Grain Size (D) (nm)	Dislocation Density (δ) ($\times 10^{-4}$)	Strain (ε) ($\times 10^{-4}$)
350	23.217	0.009669	3.8264	22.6	19.57	4.9
750	23.326	0.005236	3.8132	40.7	6.03	2.66
1050	23.107	0.003491	3.8457	56.7	3.11	1.76

3. Results and discussion

3.1 Structural analysis

The XRD pattern of the Te thin films shows the presence of the both Te and TeO_2 as shown in Fig. 2. The films are polycrystalline in nature with hexagonal structure [15, 16]. The XRD pattern of the thicker film (1050 nm) shows that the crystallites orientations parallel to c-axis with the (100) and (110) planes. The diffraction angle corresponding to the (100) and (110) planes was 23.1 and 40.6° respectively (JCPDS file no 36-1452) [15-17]. The XRD pattern of 1050 nm has (100) plane corresponding to Te having high intensity whereas the films with lower thickness shows the presence of TeO_2 peak with high intensity along with the peak corresponding to Te.

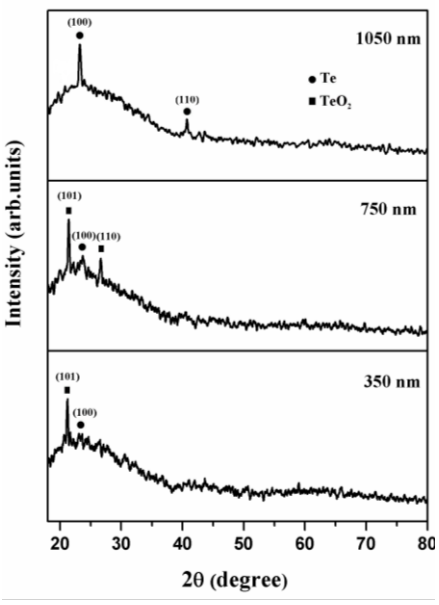

Fig. 2. XRD pattern of the Te films of different thickness.

The crystallites size were determined with Scherrer formula, [18]

$$D = 0.9\lambda / \beta\cos\theta \quad (1)$$

where, D is the grain size, λ is the wavelength (Å), β is the full width half maxima (radians) and θ is the diffraction angle (radians). The grain size obtained from XRD was 22.6, 40.0 and 56.7 nm for the thickness 350, 750 and 1050 nm respectively. Similar kind of increase in the grain size upon increasing the thickness and deposition temperature was observed in other II-VI semiconducting films also [19-21].

The Dislocation density was found using the formula [22],

$$\delta = 1 / D^2 \quad (2)$$

where, δ is the dislocation density.

It has been observed that as the thickness of the film increases the preferential (100) plane peak intensity also increases. The lattice constant a of the Te film with 1050 nm was 4.4406 Å [16]. The strain (ε) was calculated using the formula [18],

$$\varepsilon = \beta\cos\theta / 4 \quad (3)$$

where, ε is the strain, β is the full width at half maxima (FWHM) and θ is the diffraction angle.

The FWHM was found to be decrease with increasing film thickness. The decrease in FWHM reflects in the increase in lattice perfection or decrease in lattice imperfection which is due to the decrease in micro-strain and also increase in grain size [18]. Dislocation density is also decreasing with increase in the thickness. Since dislocation density is inversely proportional to the film thickness [23].

The Te films with thickness 350 and 750 nm showed TeO_2 peak along with the peaks for Te. This is because Te can readily form oxide in ambient condition as soon as it is exposed to the air [24]. Another reason this could be, even though the deposition was carried out at 10^{-5} mbar, there may be presence of oxygen and also other gases which oxidizes the film and also as the thickness of the film increases the loosely bound oxygen may get removed from the surface thus shows the Te planes. The higher thickness

film (1050 nm) showed the presence of Te peaks alone and the oxide formation was not observed. A plausible reason for this is, "new grains are nucleated on top of the old ones after a certain thickness has been reached. Nucleation of a new grain may become necessary because of a layer of contamination making coherent growth with the grain below impossible or if the top surface of the grain below is nearly perfect closed-packed plane" [25].

3.2 Morphological properties

Fig. 3 (a – g) shows the FE-SEM micrographs of Te films with different thicknesses. The grain size observed from FE-SEM was in good agreement with that of the values calculated from XRD. The micrographs also show that as the film thickness increases the homogeneity of the film increases. Uniform distribution of strip like structure was observed for the 350 nm thick Te films as shown in Figs. 3 (a & b). Also for the Te films with 750 nm thickness Fig. 3 (c) we observed the growth of granule like structure over the strip like structure and also the granule like structure alone on two different areas of the film Figs. 3 (d & e). And we observed granule structure on the entire film surface for the films with thickness 1050 nm as shown in Figs. 3 (f & g).

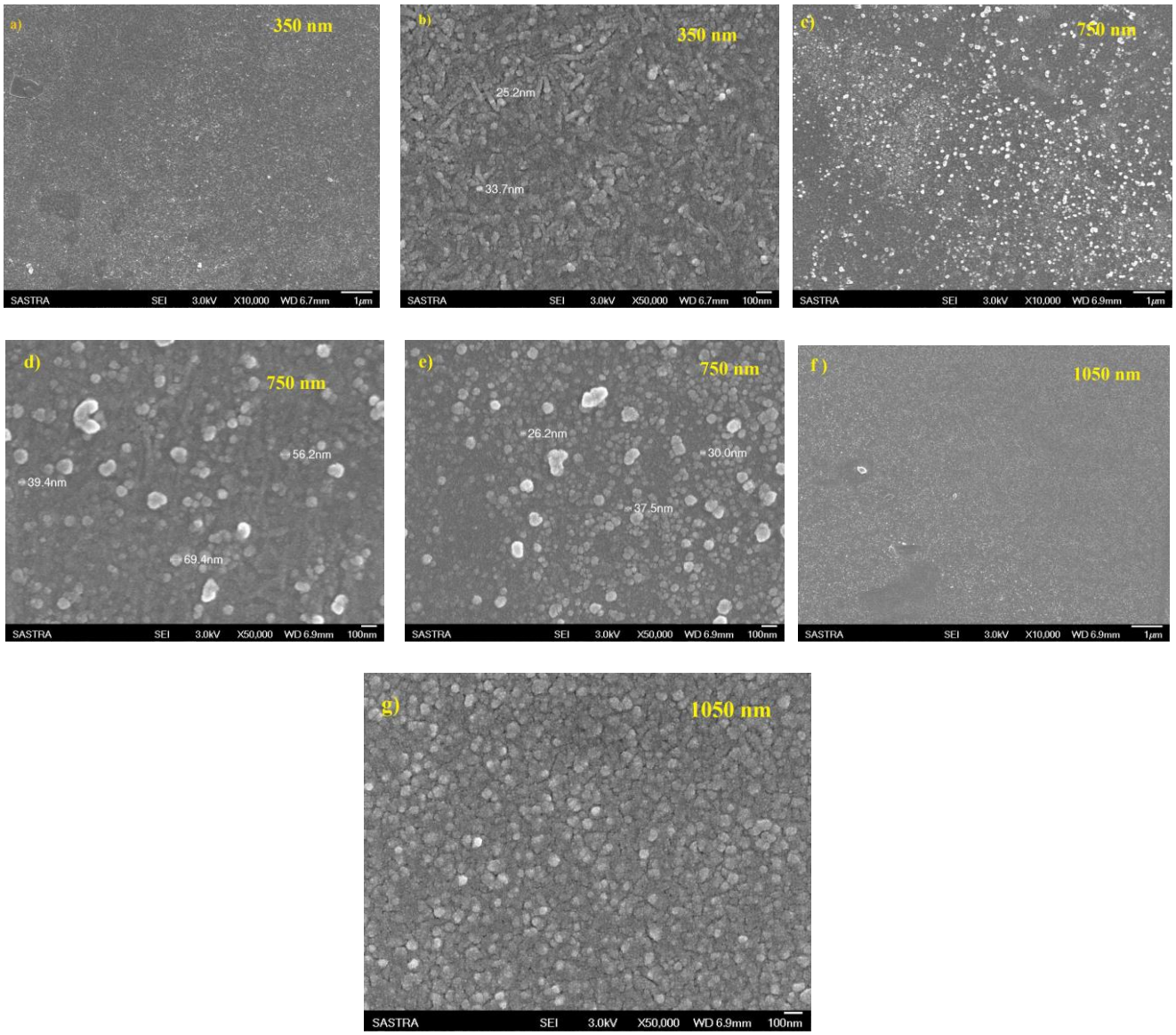

Fig. 3. (a – g) FE-SEM micrographs of Te films of different thickness.

3.3 Optical properties

Figs. 4 (a & b) shows the optical absorption and transmission spectra of the films with different thickness. The reflectance was calculated from the absorption and transmission spectra using the formula

$$R = 1 - (A + T) \tag{4}$$

where, R is the reflectance, A is the absorbance and T is the transmittance.

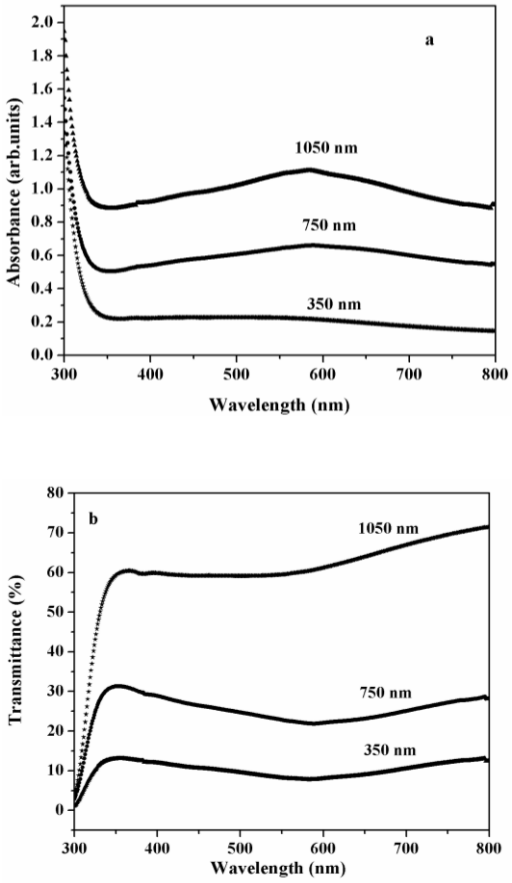

Fig. 4. Absorbance and transmission spectra of Te films of different thickness.

The optical band gap was calculated using the fundamental absorption of energy which corresponding to the electron excitation from the upper part of the valence band to the lower part of the conduction band. Band gap energy is mainly depend the absorption co-efficient and the photon energy it is given by the relation [26]

$$(\alpha h\nu)^n = A(h\nu - E_g) \tag{5}$$

where, α is the absorption coefficient, E_g is the band gap, $h\nu$ is the photon energy and A is the constant exponent. The optical band gap was obtained by the slope intercepting in X-axis for the plot $(\alpha h\upsilon)^2$ against $h\nu$ and the values were found to be 3.92, 3.78 and 1.33 eV for the films with thickness 350, 750 and 1050 nm respectively Figs. 5 (a – c). The optical band gap decreases with increase in the film thickness. This may be due to the increase in the crystallite size. When the grain size increase the grain boundary decreases, therefore free electrons trapped in the grain boundaries are reduced which in turn reduce the band gap energy [27]. From the SEM micrographs, it is observed that the grain boundaries reduce with increase in the thickness of the films. This could be a possible reason for the decrease in the band gap energy and also due to the decrease in defects with the increase in film thickness.

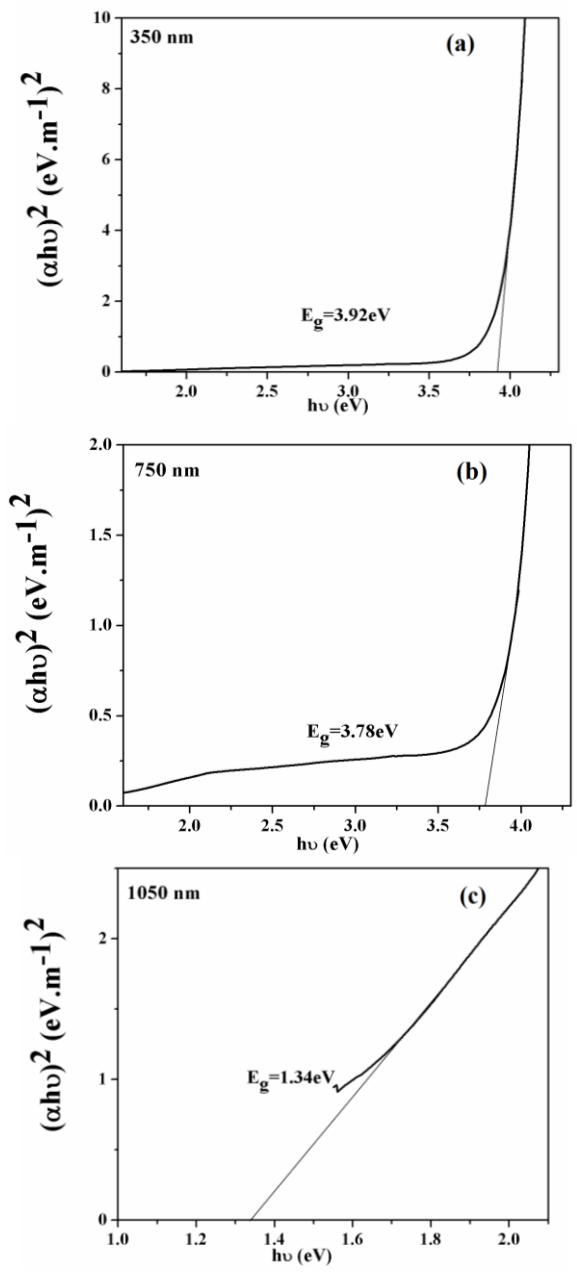

Fig. 5. Optical band gap of Te films with thicknesses a) 350 b) 750 and c) 1050 nm.

Fig. 6 shows a plot between the absorption coefficient and the photon energy. The absorption coefficient of the films were found using the formula,

$$\alpha = 2.303At \tag{6}$$

where, α is the absorption coefficient, A is the absorbance and t is the thickness of the film. The absorption coefficient of the film increases from 1×10^6 to 2×10^6 as the thickness of the film increases.

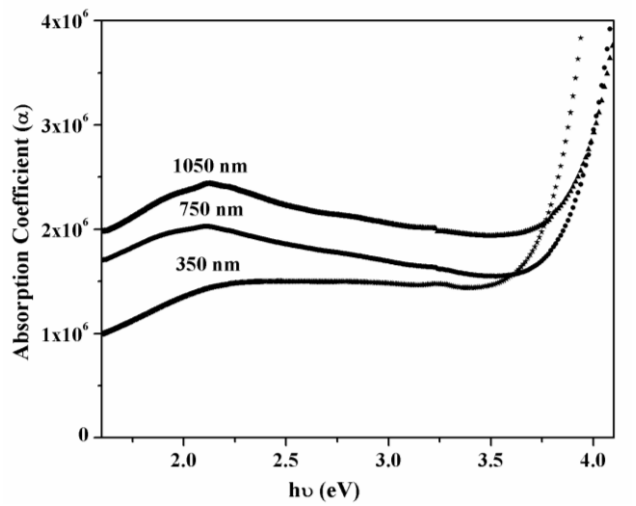

Fig. 6. Absorption coefficient (vs) photon energy plot of Te films.

The extinction coefficient is calculated from the formula

$$k = \alpha\lambda / 4\pi \tag{7}$$

where, k is the extinction coefficient, α is the absorption coefficient, λ is the wavelength.

Fig. 7. shows a plot between the extinction coefficient and the photon energy which shows the extinction coefficient value was increased from 0.06 to 0.12 as the thickness of the increases. This is because as the thickness increases roughness in the film increases which in turn results in more scattering of light. The refractive index of the film increase with increase in the thickness and the refractive index can be derived as

$$n = Abs(1+\sqrt{R})/(1-\sqrt{R}) \tag{8}$$

where, n is the refractive index and R is the reflectance

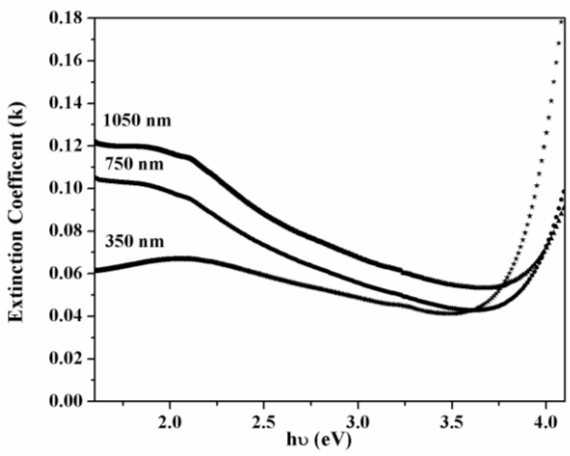

Fig. 7. Extinction coefficient (vs) photon energy plot of Te films.

Fig. 8 shows a comparison of refractive index with that of the thickness. The refractive index of the films varies from 1.25 to 1.75 as a function of thickness. The optical constant such as refractive index (n), extinction coefficient (k) and absorption coefficient (α) are always in reciprocal to that of the transmittance value [28]. So as the transmittance value of the film lowers all the other optical constants value increases.

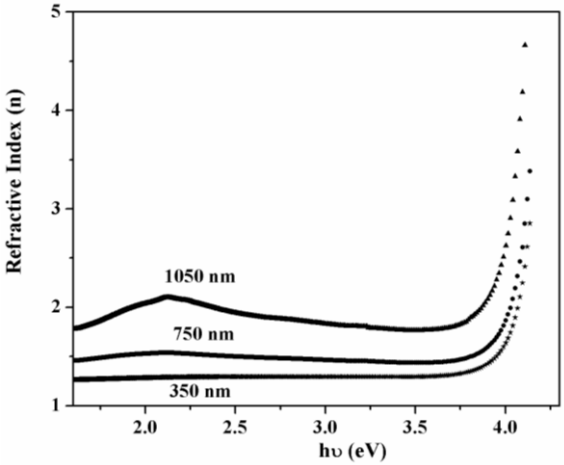

Fig. 8. Refractive index (vs) photon energy plot of Te films.

4. Conclusion

Te thin films of different thickness were coated on to the glass substrate and the effect of films thickness on structural, optical and morphological properties were studied. On increasing the thickness of the films the grain size of the films increased and the strain value decreased. The optical band gap of the film reduced from 3.92 to 1.33 eV with increase in thickness due to decrease in the lattice defects.

Acknowledgement

Authors are grateful to SASTRA University for providing the infrastructure facilities and financial support. Authors thank Dr. N. Lakshminarayan, MCC, Chennai for valuable discussions.

References

[1] T. Siciliano, M. Di Giulio, M. Tepore, E. Filippo, G. Micocci, A. Tepore, Sens. Actuators, B **135**, 250 (2008).
[2] T. Siciliano, M. Di Giulio, M. Tepore, E. Filippo, G. Micocci, A. Tepore, Sens. Actuators, B **137**, 644 (2009).
[3] Ranu Nayak, Vinay Gupta, A. L. Dawar, K. Sreenivas, Thin Solid Films **445**, 118 (2003).
[4] T. Balasubramaniam, Sa. K. Narayanadass, D. Mangalaraj, Bull. Mater. Sci. **20**, 79 (1997).
[5] M. Rusu, J. Optoelectron. Adv. Mater. **3**, 867 (2001).
[6] Alexis De Vos, Jan Aerts, Thin Solid Films **46**, 223(1977).
[7] D. Tsiulyanu, S. Marian, H. D. Leiss, I. Eisele, J. Optoelectron. Adv. Mater. **5**, 1349 (2003).
[8] D. Tsiulyanu, O. Mocreac, Journal of Non Oxide Glasses **3**, 37 (2011).
[9] Bianchetti, M. F. Heredia, E. Oviedo, C. Walsoe de reca, N. E., The Journal of Argentine Chemical Society **93**, 27 (2005).
[10] N. Lakshminarayan, M. Radhakrishnan and C. Balasubramanian, J. Mater. Sci. **21**, 246 (1986)
[11] Wen-Yaung Lee, R. H. Geiss, J. Appl. Phys. **54**, 1351 (1983).
[12] Janan H Saadee, J. Kufa – Physics **3**, 24 (2011).
[13] N. Lakshminarayan, M. Radhakrishnan and C. Balasubramanian, J. Mater. Sci. **19**, 2368 (1984).
[14] S. N. B. Hodgson, L. Weng, J. Sol-Gel Sci. Techn. **18**, 145 (2000).
[15] Paritosh Mohanty, Jeunghee Park and Bongsoo Kim, J. Nanosci. Nanotechnol. **6**, 1 (2006).
[16] Jun u, Yi Xie, Fen Xu, Liying Zhu, J. Mater. Chem. **12**, 2755 (2002).
[17] L. Weng, S. N. B. Hodgson, Optical Materials **19**, 313 (2002).
[18] Ziaul Raza Khan, M. Zulfequar, Mohd. Shahid Khan, Chalcogenide Letters. **7**, 431 (2010).
[19] M. G. Sridharan, Sa. K. Narayandass, D. Mangalaraj H. C. Lee, J. Optoelectron. Adv. Mater. **7**, 1483 (2005)
[20] M. G. Sridharan, M. Mekaladevi, Sa.K. Narayandass, D. Mangalaraj, H. C. Lee, J. Optoelectron. Adv. Mater. **7**, 1479 (2005).
[21] M. Sridharan, Sa. K. Narayandass, D. Mangalaraj, H. C. Lee, Vacuum. **68**(2), 119 (2002).
[22] S. Lalitha, R. Sathyamoorthy, S. Senthilarasu, A. Subbarayan, K. Natarajan, Solar Energy Materials & Solar Cells **82**, 187 (2004).
[23] Masami Tachikawa and Masafumi Yamaguchi, Appl. Phys. Lett. **56**, 184 (1990).
[24] Shashwati Sen, K. P. Muthe, Niraj Joshi, S. C. Gadkari, S. K. Gupta, Jagannath, M. Roy, S. K. Deshpande, J. V. Yakhmi, Sens. Actuators, B **98**, 154 (2004).
[25] Leon I. Maissel, Reinhard Glang, Handbook of thin film technology, McGraw-Hill, Inc. (1983).
[26] J. Tauc, Studies of the band tails in a-Si:H by photomodulation spectroscopy, Sol. Energy Mater. **8**, 259 (1982).
[27] Monjoy Sreemany, Ankila Bose, Suchitra Sen, Physica B **405**, 85 (2010).
[28] A. Abdolahzadeh Ziabari, F. E. Ghodsi, J Mater Sci: Mater Electron **23**, 1628 (2012).

*Corresponding author: m.sridharan@ece.sastra.edu